

PAPER • OPEN ACCESS

Instability of adiabatic shear flows in a channel

To cite this article: A Barletta *et al* 2024 *J. Phys.: Conf. Ser.* **2685** 012073

View the [article online](#) for updates and enhancements.

You may also like

- [Application of Arnoldi method to boundary layer instability](#)
Yong-Ming Zhang, , Ji-Sheng Luo et al.
- [An optimization approach for analysing nonlinear stability with transition to turbulence in fluids as an exemplar](#)
R R Kerswell, C C T Pringle and A P Willis
- [A new mathematical model of rigid boundary in shear flows](#)
R Chanishvili, G Chagelishvili, M Kalashnik et al.



ECS
The
Electrochemical
Society
Advancing solid state &
electrochemical science & technology

DISCOVER
how sustainability
intersects with
electrochemistry & solid
state science research

Instability of adiabatic shear flows in a channel

A Barletta^{1,*}, M Celli¹, S Lazzari², P V Brandão¹

¹ Department of Industrial Engineering, Alma Mater Studiorum Università di Bologna, Bologna, Italy

² Department of Architecture and Design, University of Genoa, Stradone S. Agostino 37, 16123 Genoa, Italy

* email: antonio.barletta@unibo.it

Abstract. The combined forced and free convection flow of a Newtonian fluid in a horizontal plane-parallel channel is examined. The boundary walls are considered as adiabatic, so that the only thermal effect acting in the fluid is the viscous dissipation due to the nonzero shear flow. As the shear flow may be caused by either an imposed horizontal pressure gradient or an imposed velocity difference between the bounding walls, one may envisage two scenarios where the stationary basic flow is Poiseuille-like or Couette-like, respectively. Both cases are surveyed with a special focus on practically significant cases where the Gebhart number is considered as very small, though nonzero. Furthermore, the Prandtl number is assumed as extremely large, thus pinpointing a scenario of creeping buoyant flow with a fluid having a very large viscosity. Within such a framework, the instability of the basic flow is analysed versus small-amplitude perturbations.

Keywords: *Channel flow, Buoyancy, Viscous dissipation, Shear flows, Linear stability*

1. Introduction

The viscous dissipation contribution to the local energy balance for a fluid can influence the heat transfer and flow features for internal flows. It is well-known in the literature that significant effects of viscous dissipation may be present in either forced or mixed convection. On the other hand, such effects are generally less intense in a regime of natural convection [1].

Starting from the paper by Joseph [2], the question on whether viscous dissipation might be the source of instability for internal fluid flows was posed. Joseph [2] built up a model where the instability mechanism arises from a combined action of the viscous dissipation term in the local energy balance and the viscous force in the local momentum balance activated through the temperature-dependence of the fluid viscosity. A different approach has been proposed more recently by Barletta [3]. The idea is that the buoyancy force in a mixed convection regime can be the term providing the thermal interaction within the local momentum balance. Roughly speaking, such a different approach replaces the variable-viscosity coupling with a variable-density coupling between the energy and momentum balances. In particular, the variable-density coupling is modelled via the classical Boussinesq approximation.

When the focus is on the onset of convection patterns superposed to a parallel flow in a channel, the cause of instability is generally an external forcing induced by the temperature boundary conditions at the walls. When this is the case, then the thermal instability is of the Rayleigh-Bénard type and the governing parameter driving the transition is the Rayleigh number, provided that other parameters,



such as the Prandtl number and the Reynolds number, are prescribed. Another scenario is one where no external forcing due to the temperature boundary conditions exists, yet a temperature gradient is present due to the viscous dissipation and consequent heating of the flowing fluid. This cause of thermal instability is endogenous as it is determined by the impressed flow rate associated with the stationary parallel velocity field in a channel or duct.

An interesting aspect is the possible comparison between the thermal instability induced by viscous dissipation and the well-known hydrodynamic instability of internal flows, classically studied via the analysis and solution of the Orr-Sommerfeld eigenvalue problem. The hydrodynamic instability is defined by the threshold, or critical, value of the Reynolds number predicted by the linear stability analysis. A finite critical Reynolds number exists for the Poiseuille flow in a plane channel. For the Hagen-Poiseuille flow in a circular duct or the Couette flow in a plane channel, the nonlinear analysis predicts a threshold to instability in terms of the Reynolds number, while the linear theory predicts no instability [4, 5].

The viscous dissipation is the source of an instability completely different from the hydrodynamic instability. In fact, its effects can well emerge at Reynolds numbers lower than those needed for the hydrodynamic instability [6]. Despite the thermal origin of the dissipation instability, it can display its onset under conditions of adiabatic boundary walls and with the flow itself causing the instability as mediated by the thermal coupling in the local momentum balance equation [6].

This paper will survey the study presented in Barletta et al. [6], where the buoyancy-induced steady-state modification of the Poiseuille profile in a horizontal plane channel is considered. That study [6] assumes adiabatic boundary walls and a non-negligible effect of viscous dissipation as the sole cause of the buoyancy force. The resulting velocity profiles for the basic flow depend on the Gebhart number, which is usually less or much less than unity except when large scale flows are considered, as it happens in geophysics [6]. The Gebhart number is also well-known in the geophysics literature as the dissipation parameter. It comes up whenever the interplay between viscous dissipation and thermal buoyancy proves to be important. If the focus of Barletta et al. [6] is on the dissipation instability of the adiabatic Poiseuille-like flows in a horizontal plane channel, this paper will also survey the onset of the dissipation instability for the Couette-like flows in a horizontal plane channel [7]. In the latter case, the zero-velocity boundary conditions for the velocity field are turned into no-slip conditions with a relative velocity imposed across the boundaries. The linear stability analysis will be parametrised by the Gebhart number and will turn out to be subject to an overall flow scale given by the Péclet number. A numerical solution of the stability eigenvalue problem will be carried out leading to the determination of the neutral stability curves and to the critical values of the Péclet number for the transition to instability.

2. Governing Equations

The flow in a horizontal plane channel with boundary walls separated by a distance H is described by the mass, momentum and energy local balance equations. They are written according to the Boussinesq approximation in the dimensionless form

$$\nabla \cdot \mathbf{u} = 0, \quad (1)$$

$$\frac{1}{\text{Pr}} \left[\frac{\partial \mathbf{u}}{\partial t} + (\mathbf{u} \cdot \nabla) \mathbf{u} \right] = -\nabla p + T \hat{\mathbf{e}}_z + \nabla^2 \mathbf{u}, \quad (2)$$

$$\frac{\partial T}{\partial t} + \mathbf{u} \cdot \nabla T = \nabla^2 T + \text{Ge} \Phi, \quad (3)$$

where the z axis, with unit vector $\hat{\mathbf{e}}_z$, is taken as vertical and perpendicular to the boundary walls. The Cartesian coordinates, (x, y, z) , time, t , velocity, $\mathbf{u} = (u, v, w)$, temperature, T , and pressure, p , have been made dimensionless by using, respectively, the scales:

$$H, \quad \frac{H^2}{\alpha}, \quad \frac{\alpha}{H}, \quad \frac{\alpha v}{g\beta H^3}, \quad \frac{\rho \alpha v}{H^2}, \quad (4)$$

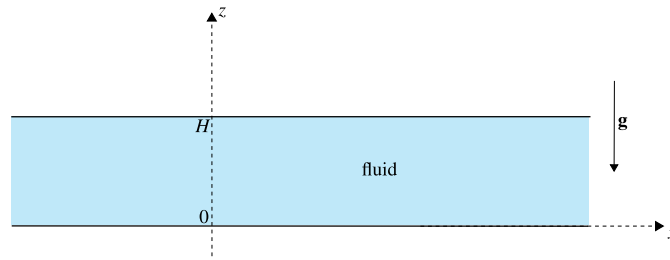


Figure 1. A sketch of the channel.

where the fluid properties α (thermal diffusivity), ν (kinematic viscosity), β (thermal expansion coefficient), ρ (density) are employed together with the modulus, g , of the gravitational acceleration, \mathbf{g} . The dimensionless parameters Pr and Ge are the Prandtl number and the Gebhart number. They are defined as

$$Pr = \frac{\nu}{\alpha}, \quad Ge = \frac{g\beta H}{c}, \quad (5)$$

with c the fluid specific heat. In Eq. (3), Φ denotes the dimensionless dissipation function,

$$\Phi = \frac{1}{2} \sum_{i,j} \left(\frac{\partial u_i}{\partial x_j} + \frac{\partial u_j}{\partial x_i} \right)^2, \quad (6)$$

where u_i is the i -th component of \mathbf{u} and x_i the i -th Cartesian coordinate.

The origin of the z axis, $z = 0$, is set at the lower boundary wall so that the upper boundary wall is at $z = 1$. A sketch of the channel with the dimensional quantities is displayed in Fig. 1.

3. Stationary Basic Shear Flows

A class of stationary two-dimensional solutions of Eqs. (1)-(3) exist in the xz plane. They can be expressed as

$$\mathbf{u}_b = \left(Pe F(z), 0, 0 \right), \quad T_b = Pe Ax + Pe^2 G(z), \quad \nabla p_b = \left(Pe F''(z), 0, T_b \right), \quad (7)$$

where the primes denote derivatives with respect to z and subscript b stands for “basic” solution. The functions $F(z)$, $G(z)$ and the constants A , Pe are determined from the boundary conditions imposed at $z = 0, 1$. We always constrain the boundaries to be thermally insulated, so that

$$\frac{\partial T_b}{\partial z} = 0 \quad \text{for } z = 0, 1. \quad (8)$$

On the other hand, we devise two cases where the momentum boundary conditions may yield either zero velocity at both boundaries,

$$u_b = 0 \quad \text{for } z = 0, 1, \quad (9)$$

or a boundary velocity difference,

$$u_b = 0 \quad \text{for } z = 0, \quad u_b = Pe \quad \text{for } z = 1. \quad (10)$$

Eq. (9) leads to a Poiseuille-like class of solutions, where the Péclet number Pe defines the dimensionless flow rate across the channel,

$$Pe = \int_0^1 u_b dz. \quad (11)$$

Eq. (10) leads to a Couette-like class of solutions, where the Péclet number yields the dimensionless velocity difference between the boundaries. The flow rate is set to zero in the inertial reference frame where the relative velocity difference between the boundaries is zero. In other words, instead of Eq. (11), we prescribe in this case

$$\frac{\text{Pe}}{2} = \int_0^1 u_b dz. \quad (12)$$

In either cases, $F(z)$ and $G(z)$ depend both on Ge and on the constant A , while they are independent of Pe . Both $F(z)$ and $G(z)$ are polynomials in z . Due to the Neumann boundary conditions for the temperature (8), $G(z)$ is determined only up to an arbitrary additive constant. Such an arbitrariness can be broken by setting $G(0) = 0$ and, hence, attributing to $G(z)$ the meaning of dimensionless temperature difference between a given z and the lower boundary, $z = 0$, for a given $x = \text{constant}$ channel cross-section.

4. Linear Instability

One can inspect the onset of the instability by perturbing the basic flow (7), namely by expressing the flow fields (\mathbf{u}, T, p) as the sum of the basic state contribution (\mathbf{u}_b, T_b, p_b) plus a perturbation (\mathbf{U}, Θ, P) , with $\mathbf{U} = (U, V, W)$. By substituting this decomposition into the governing equations (1)-(3) and by linearising with respect to the perturbations, one obtains

$$\nabla \cdot \mathbf{U} = 0, \quad (13)$$

$$\frac{1}{\text{Pr}} \left[\frac{\partial \mathbf{U}}{\partial t} + (\mathbf{u}_b \cdot \nabla) \mathbf{U} + (\mathbf{U} \cdot \nabla) \mathbf{u}_b \right] = -\nabla P + \Theta \hat{\mathbf{e}}_z + \nabla^2 \mathbf{U}, \quad (14)$$

$$\frac{\partial \Theta}{\partial t} + (\mathbf{u}_b \cdot \nabla) \Theta + (\mathbf{U} \cdot \nabla) T_b = \nabla^2 \Theta + 2\text{Ge} \left(\frac{\partial U}{\partial z} + \frac{\partial W}{\partial x} \right) u'_b, \quad (15)$$

$$\mathbf{U} = 0, \quad \frac{\partial \Theta}{\partial z} = 0 \quad \text{for } z = 0, 1, \quad (16)$$

where the boundary conditions (16) express the no-slip, impermeability and thermal insulation characteristics of the boundary walls.

A realistic regime for the onset of dissipation instability is one involving a very viscous fluid ($\text{Pr} \gg 1$). Then, the governing equations for the linear stability analysis lead to a partial differential boundary value problem in the unknowns (W, Θ) ,

$$\nabla^4 W + \frac{\partial^2 \Theta}{\partial y^2} = 0, \quad (17)$$

$$\frac{\partial \Theta}{\partial t} + \text{Pe}^2 W G'(z) = \frac{\partial^2 \Theta}{\partial y^2} + \frac{\partial^2 \Theta}{\partial z^2}, \quad (18)$$

$$W = 0, \quad \frac{\partial W}{\partial z} = 0, \quad \frac{\partial \Theta}{\partial z} = 0 \quad \text{for } z = 0, 1. \quad (19)$$

4.1. Normal Modes

According to the classical procedure, one now expresses the (W, Θ) perturbations as Fourier modes,

$$(W, \Theta) = (f(z), h(z)) e^{\lambda t} e^{iky}, \quad (20)$$

where the complex parameter $\lambda = \eta - i\omega$ defines, through its real and imaginary parts, the growth rate η and the angular frequency ω of the Fourier mode, while the real parameter k is the wavenumber. The threshold to linear instability, or neutral stability condition, is given by $\eta = 0$, while $\eta > 0$ means instability and $\eta < 0$ means linear stability. The forthcoming analysis will show that, both in the case

of Poiseuille-like flows obtained by imposing Eqs. (9) and (11) and in the case of Couette-like flows obtained by imposing Eqs. (10) and (12), $G'(z)$ turns out to be proportional to the Gebhart number when this parameter is very small. Thus, we can define a function $q(z)$ as

$$\lim_{\text{Ge} \rightarrow 0} \frac{G'(z)}{\text{Ge}} = q(z). \quad (21)$$

One is lead to the conclusion that the realistic small-Ge regime is to be accomplished with a large Péclet number in order to describe the onset of the instability. More precisely, the double limit $\text{Ge} \rightarrow 0$ and $\text{Pe} \rightarrow \infty$ must be taken with the constraint that GePe^2 is kept finite or, equivalently,

$$\mathcal{R} = \text{Pe} \sqrt{\text{Ge}} \sim \text{O}(1). \quad (22)$$

Bearing this result in mind, the $\text{Ge} \rightarrow 0$ and $\text{Pe} \rightarrow \infty$ the linear stability eigenvalue problem is given by

$$f'''' - 2k^2 f'' + k^4 f - k^2 h = 0, \quad (23)$$

$$h'' - (k^2 + \lambda) h - \mathcal{R}^2 q(z) f = 0, \quad (24)$$

$$f = 0, \quad f' = 0, \quad h' = 0 \quad \text{for } z = 0, 1. \quad (25)$$

Eqs. (23)-(25) define the stability eigenvalue problem for the limiting case of small Gebhart number. Thus, the neutral stability condition may be expressed through a k -dependent value of \mathcal{R} , where the minimum of \mathcal{R} over all the allowed wavenumbers k yields the critical condition: $k = k_c$ with $\mathcal{R} = \mathcal{R}_c$.

4.2. Numerical Solver

One can determine numerically the solution of Eqs. (23)-(25) by employing the shooting method (see, for instance, chapter 10 of Barletta [8]). This technique requires the original eigenvalue problem to be reshaped from its original homogeneous statement, Eqs. (23)-(25), into a non-homogeneous form that filters out the trivial solutions, $f(z) = 0$ and $h(z) = 0$, by breaking the scale-invariance of the eigenfunctions, *i.e.*, the functions $f(z)$ and $h(z)$. In practice, this step requires the introduction of a new boundary condition, say, $h(0) = 1$ and the exclusion of one of the conditions (25), say, $h'(1) = 0$. While the resulting inhomogeneous boundary value problem yields a non-trivial determination of the eigenfunctions $f(z)$ and $h(z)$ for every assignment of the parameters $(k, \lambda, \mathcal{R})$, one can employ the excluded condition $h'(1) = 0$ to determine the complex eigenvalue λ . The numerical determination of λ means the evaluation of the growth rate, η , and of the angular frequency, ω . If the former parameter allows one to place the locus of neutral stability ($\eta = 0$), the latter parameter results to be zero in every case of neutral stability examined, thus meaning that the longitudinal rolls do not travel along the y direction.

5. Poiseuille-like Flows

We refer the reader to Barletta et al. [6] for an explicit expression of $F(z)$ and $G(z)$ in the case of the Poiseuille-like flows when Eqs. (9) and (11) are employed. We just mention that we have a two-fold determination of the constant A for every fixed value of Ge , independently of the Péclet number,

$$A = A_{\pm} = 24 \frac{15 \pm \sqrt{15(15 - \text{Ge}^2)}}{\text{Ge}}. \quad (26)$$

This result implies a two-fold determination of the velocity, temperature and pressure profiles (7) where, however, the branch $A = A_+$ turns out to be unphysical for the sufficiently small values of Ge characteristic of most engineering applications [6]. Thus, by taking $A = A_-$ and by assuming $\text{Ge} \ll 1$, one gets the approximate expressions

$$F(z) \approx 6z(1-z) + \text{Ge}z(1-z)(1-2z) + \text{O}(\text{Ge}^2), \quad G(z) \approx -18\text{Ge}z^2(1-z)^2 + \text{O}(\text{Ge}^2). \quad (27)$$

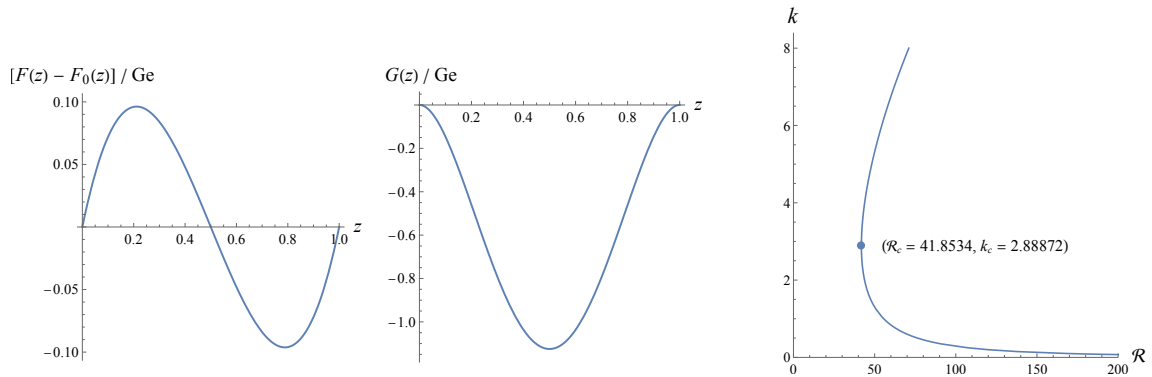


Figure 2. Poiseuille-like flows: incremental velocity profile, temperature profile for $Ge \ll 1$ and neutral stability curve in the (\mathcal{R}, k) plane.

It is evident from Eq. (27) that, when $Ge \rightarrow 0$, Eq. (7) yields the classical Poiseuille velocity profile for the isothermal fluid flow in a channel, $F(z) = F_0(z) = 6z(1-z)$ with $G(z) = 0$ and $A = 0$. Discrepancies with respect to such isothermal flow conditions are illustrated in Fig. 2 for a regime where $Ge \ll 1$. In particular, one may figure out that the effect of viscous dissipation produces an asymmetry of the velocity profile with the maximum slightly shifted from the midplane $z = 1/2$. Furthermore, Fig. 2 reveals a potentially unstable thermal stratification in the lower half-channel, with the midplane temperature smaller than the boundary temperature at a fixed x .

On account of Eqs. (21) and (27), one obtains, in this case, the expression of function $q(z)$,

$$q(z) = -36z(1-z)(1-2z). \quad (28)$$

One may substitute Eq. (28) into the eigenvalue problem (23)-(25) and use the numerical solution technique described in Section 4.2. Thus, as already anticipated in Section 4.2, one obtains that the angular frequency ω of the neutrally stable modes is zero. Furthermore, the neutral stability curve can be plotted in the (\mathcal{R}, k) plane as shown in Fig. 2. As displayed in Fig. 2, the minimum of \mathcal{R} along the neutral stability curve is achieved with $\mathcal{R} = \mathcal{R}_c$ and $k = k_c$, where

$$\mathcal{R}_c = 41.8534, \quad k_c = 2.88872. \quad (29)$$

Eq. (29) identifies the critical point for the onset of the linear instability [6]. An important feature of the neutral stability curve displayed in Fig. 2 is that there is no finite limit for \mathcal{R} at neutral stability when $k \rightarrow 0$.

6. Couette-like Flows

In the case where Eqs. (10) and (12) are imposed, we are led to Couette-like flows [7]. In particular, we have

$$A = A_{\pm} = 12 \frac{15 \pm \sqrt{5(45 - Ge^2)}}{Ge}. \quad (30)$$

As for the Poiseuille-like flows discussed in Section 5, also in this case we have just one physically acceptable solution, namely $A = A_-$, for the regime of small Gebhart numbers. With this choice of the constant A , the approximate solution for $Ge \ll 1$ is given by

$$F(z) \approx z + \frac{1}{6} Ge z(1-z)(1-2z) + O(Ge^2), \quad G(z) \approx -\frac{1}{6} Ge z^2(3-2z) + O(Ge^2). \quad (31)$$

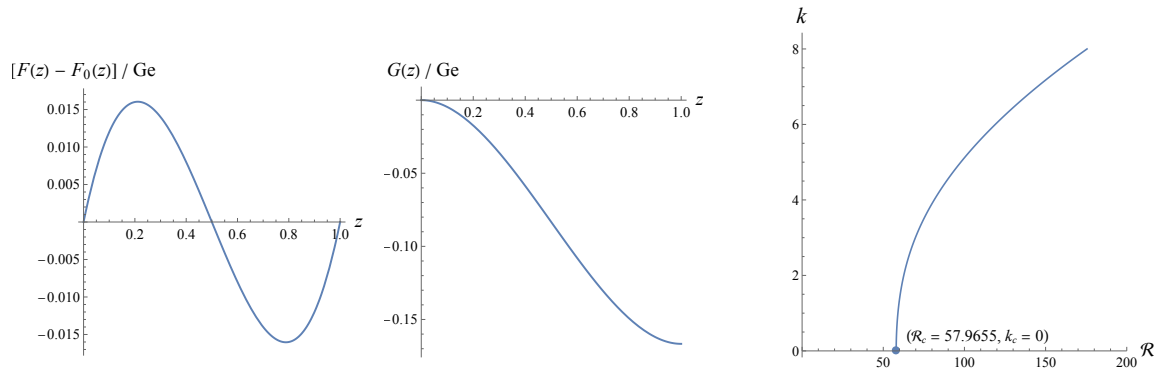


Figure 3. Couette-like flows: incremental velocity profile, temperature profile for $Ge \ll 1$ and neutral stability curve in the (\mathcal{R}, k) plane.

The obvious consequence of Eqs. (7) and (31) is that the limit $Ge \rightarrow 0$ of the basic velocity profile is the classical isothermal Couette flow in a plane channel, defined by $F(z) = F_0(z) = z$ with $G(z) = 0$ and $A = 0$. The linear velocity profile of the Couette flow is slightly altered by the buoyancy effect of viscous dissipation with larger local values of velocity in the lower half-channel ($z < 1/2$) and slightly smaller velocities in the upper half-channel ($z > 1/2$). This behaviour is displayed in Fig. 3, where also the temperature profile in a $x = \text{constant}$ cross-section is displayed. Differently from the case of the Poiseuille-like flows illustrated in Section 5, Fig. 3 shows that the z component of the temperature gradient is always negative. The consequence is a potentially unstable thermal stratification throughout the whole channel.

By employing Eqs. (21) and (31), one may determine function $q(z)$ needed for a complete formulation of the stability eigenvalue problem (23)-(25), namely

$$q(z) = -z(1-z). \quad (32)$$

Again, one may employ the numerical solver presented in Section 4.2. As pointed out in Section 4.2, one evaluates again a zero angular frequency ω for all the neutrally stable modes. Moreover, one can display the neutral stability curve in the (\mathcal{R}, k) plane as plotted in Fig. 3. Differently from the case of the Poiseuille-like flows, the minimum of \mathcal{R} along the neutral stability curve is achieved when $k \rightarrow 0$, so that

$$\mathcal{R}_c = 57.9655, \quad k_c = 0. \quad (33)$$

Interestingly enough, the infinite wavelength modes, ineffective for the onset of the instability in the case of the Poiseuille-like flows, are the most unstable when one considers the Couette-like flows.

7. Critical Reynolds Number

The stability analysis carried out so far identifies \mathcal{R} , defined by Eq. (22), as the parameter governing the transition from the basic parallel flow to the cellular convection flow in the channel. A more inspiring statement of the transition to instability can be made in terms of the Reynolds number, $Re = Pe/Pr$, as this parameter allows an easy comparison with the hydrodynamic instability driven by the Tollmien-Schlichting modes [9]. Eqs. (29) and (33) yield a critical condition for the Reynolds number expressed as

$$Re_c = \begin{cases} 41.8534 Pr^{-1} Ge^{-1/2}, & \text{Poiseuille-like flows,} \\ 57.9655 Pr^{-1} Ge^{-1/2}, & \text{Couette-like flows.} \end{cases} \quad (34)$$

Obviously, any comparison with the hydrodynamic instability is possible only when Pr and Ge are prescribed. Due to their definitions, Eq. (5), this is possible only for a given fluid and a given value of the vertical width H . Then, we can imagine an experimental setup where $H = 10^{-2}$ m and the working fluid is glycerine at 300 K (data provided in Ref. [10]). By using Eq. (5), we obtain $Ge = 1.94 \times 10^{-8}$, so that Eq. (34) yields

$$Re_c = \begin{cases} 44.3, & \text{Poiseuille-like flow,} \\ 61.4, & \text{Couette-like flow.} \end{cases} \quad (35)$$

The linear transition to hydrodynamic instability happens with $Re_c = 5772.22$ for the plane Poiseuille flow, while Re_c is infinite for the plane Couette flow [9]. Thus, Eq. (35) reveals that the dissipation instability induced by the buoyancy force acts at significantly lower Reynolds number with respect to the hydrodynamic instability.

8. Conclusions

A family of stationary and parallel shear flows in a horizontal plane channel have been studied. Such flows are solution of the governing balance equations for fluid flow under the Boussinesq approximation by taking into account the viscous dissipation effect. The channel boundaries are considered as adiabatic and subject to either Poiseuille-like or Couette-like velocity conditions. In the first case, the flow is sustained by an imposed horizontal pressure gradient. In the second case, the cause of the flow is the velocity difference between the boundaries. In all cases, the only thermal effect generating a nonzero temperature gradient is the viscous dissipation due to the fluid flow. The onset of the linear instability of the parallel shear flows has been investigated under the assumptions of a very small Gebhart number, Ge , and a very large Prandtl number, Pr . The results surveyed in this paper are important for several engineering applications where the dissipation of energy as heat can have significant implications for the design and performance of devices. In fluid transport systems, like pipelines, viscous dissipation can cause a temperature rise in the fluid. This temperature increase can affect the thermophysical properties of the fluid, such as the viscosity and density, which can, in turn, impact the performance and require additional thermal design solutions. In minifluidic or microfluidic devices, where the characteristic length scales are small, viscous dissipation can become a significant factor. It can lead to non-uniform temperature distributions within the fluid, affecting the chemical reactions, the flow rates, and the mixing processes.

Acknowledgement

The authors acknowledge financial support from Italian Ministry of Education, University and Research (MIUR) grant number PRIN 2017F7KZWS.

References

- [1] Gebhart B 1962 *Journal of Fluid Mechanics* **14** 225–232
- [2] Joseph D D 1964 *The Physics of Fluids* **7** 1761–1771
- [3] Barletta A 2015 *International Journal of Thermal Sciences* **88** 238–247
- [4] Joseph D D and Carmi S 1969 *Quarterly of Applied Mathematics* **26** 575–599
- [5] Romanov V A 1973 *Functional Analysis and its Applications* **7** 137–146
- [6] Barletta A, Celli M and Rees D A S 2023 *Physics of Fluids* **35** 033111
- [7] Barletta A, Celli M, Lazzari S and Brandão P V 2023 *International Journal of Thermal Sciences* **194** 108571
- [8] Barletta A 2019 *Routes to Absolute Instability in Porous Media* (Springer)
- [9] Drazin P G and Reid W H 2004 *Hydrodynamic Stability* 2nd ed (Cambridge University Press)
- [10] Bergman T L, Lavine A S, Incropera F P and DeWitt D P 2011 *Fundamentals of Heat and Mass Transfer* 7th ed (John Wiley & Sons)